

Non-standard neutrino interaction induced by conformal coupling

H. Yazdani Ahmadabadi* and H. Mohseni Sadjadi†

Department of Physics, University of Tehran,
P. O. B. 14395-547, Tehran 14399-55961, Iran

January 11, 2022

Abstract

A modified neutrino flavor conversion is studied within the framework of screening models through their conformal couplings to a scalar field. Such a coupling results in a new interaction between the scalar field and neutrinos. We study the discrepancy in the total flux of solar electron-neutrinos through this interaction. As the behavior of the scalar field depends on the local matter density, we see an indirect effect of matter on the flavor change. We discuss the MSW effect in this framework. The paper ends by comparing the results with the observational data.

1 Introduction

Most of the observational neutrino flavor conversion data from various experiments such as Super-Kamiokande (SK) [1], Sudbury Neutrino Observatory (SNO) [2] and KamLAND [3] can be accommodated and analyzed within the three-neutrino oscillation framework. Along their path towards detectors, neutrinos propagate through the vacuum or matter. For neutrinos traveling in the vacuum, the Schrödinger-like equation describing neutrino oscillations can be solved precisely, resulting in the phase of oscillations [4–12]. However, when neutrinos propagate in the matter, neutrinos flavor change is affected by their forward elastic scattering from solar electrons (i.e., caused by the standard weak interactions). An effective matter potential describes its effect due to the Mikheyev-Smirnov-Wolfenstein (MSW) effect [13, 14], which is an adiabatic flavor conversion in a medium with slowly varying mass density and can dramatically impact the neutrino oscillation phenomenon [15].

Discovering the properties of neutrinos is a fundamental goal in exploring physics beyond the standard model (BSM) and understanding the Universe. In contrast to the standard model's (SM) prediction, the neutrino oscillation process has indicated that neutrinos have non-zero masses. This experimentally confirmed fact has motivated people to look for other neutrino features BSM, e.g., the new unknown interactions [13, 16–18]. These additional non-standard interactions (NSI) between neutrinos and other components may modify the neutrino evolution inside matter through an effective potential that alters the neutrino mass and mixing parameters.

Neutrino-exotic field with NSI plays a crucial role in cosmology [19–23]. These fields may be used as the dark energy component of the Universe to describe the present cosmic acceleration. The motivation for coupling between dark energy and neutrinos is that the energy scale of dark energy is similar to the neutrino mass scale [20, 24]. In neutrino mass varying models [25–31], the neutrinos and a scalar field are linked to each other by the neutrino mass, which has roots in the dark energy model. The dependence of the neutrino mass on the environment due to the interactions with dark sectors demonstrates that the NSI affects the oscillations formulas [11, 32].

In some scalar-tensor dark energy models, a quintessential field interacts with matter components through a conformal coupling [33–35]. This coupling may give rise to the screening effect as was studied in the chameleon model [36–40]. In this model, the scalar field mass is an increasing function of the ambient matter density, which allows the field to screen itself in dense regions.

*hossein.yazdani@ut.ac.ir

†mohsenisad@ut.ac.ir

The outline of the paper is as follows: In section 2, we develop the idea of neutrino flavor change affected by neutrino-scalar field conformal coupling starting with the neutrino action, including the interacting part inside matter. We explicitly calculate the effective scalar-dependent mass, the wavefunction, and the weak Fermi parameter. We then obtain effective mass and mixing parameters by diagonalizing the effective neutrino Hamiltonian. We will discuss the possibility of neutrino decay and deficit in the total probability in section 3. Furthermore, we obtain various damped transition probabilities in this section. Results and their discussions are presented in section 4. We will compare our results to the Borexino data [41] for the large mixing angle (LMA) MSW survival probability. In the appendix, we give the analytical solutions to the chameleon scalar field equations, both inside and outside of the body, and discuss how the field evolves as a function of the fractional radius in the presence of the solar matter.

Throughout this paper we will use units $\hbar = c = 1$, and metric signature $(-, +, +, +)$.

2 Modified neutrino characteristics from conformal coupling

The neutrino standard interaction (SI) is associated with $\nu_e e^-$ interactions through the charged weak currents. In addition, the non-standard couplings to a scalar field can modify the effective neutrino mixing parameters and consequently transition probabilities inside matter.

We start by considering an action in which a scalar field ϕ couples to different matter fields Ψ_i by definition [42, 43]

$$\tilde{g}_{\mu\nu}^{(i)} = A_i^2(\phi)g_{\mu\nu}, \quad (1)$$

that is,

$$S_\phi = \int d^4x \sqrt{-g} \left[\frac{M_p^2}{2} \mathcal{R} - \frac{1}{2} g^{\mu\nu} \partial_\mu \phi \partial_\nu \phi - V(\phi) \right] + \int d^4x \mathcal{L}_m(\Psi_i, \tilde{g}_{\mu\nu}^{(i)}), \quad (2)$$

where g is the determinant of the metric $g_{\mu\nu}$, M_p is the reduced Planck mass, \mathcal{R} is the Ricci scalar, $V(\phi)$ is the scalar field potential, and \mathcal{L}_m is the Lagrangian density of matter components. In this work, we assume that the non-relativistic matter is universally coupled to the metric $\tilde{g}_{\mu\nu}$. On the other side, we can generalize this to the various arbitrary functions $A_i(\phi)$ for each matter component, which leads us to the violation of the weak equivalence principle (WEP) in cosmological scales [37, 38, 40]. We write the coupling function $A(\phi)$ in an exponential form, i.e., we have

$$A(\phi) = \exp \left[\frac{\beta \phi}{M_p} \right], \quad (3)$$

where β denotes the matter-scalar coupling strength. Theories with $\beta \sim 1$ have gravitational strength couplings to matter [40], whereas the $\beta \rightarrow 0$ reproduces the no-chameleon case.

Including the interacting term, we have the following fermionic action [44]:

$$\begin{aligned} \tilde{S}_\nu^m = \int d^4x \sqrt{-\tilde{g}} \left[- \sum_{\alpha, \beta} \nu_{\alpha L}^\dagger m_{\alpha\beta} \nu_{\beta R} - \sum_{\alpha, \beta} \nu_{\alpha R}^\dagger m_{\beta\alpha}^* \nu_{\beta L} \right. \\ \left. + i \sum_{\alpha} \left(\nu_{\alpha L}^\dagger \tilde{\sigma}_L^\mu \tilde{D}_\mu \nu_{\alpha L} + \nu_{\alpha R}^\dagger \tilde{\sigma}_R^\mu \tilde{D}_\mu \nu_{\alpha R} \right) - 2\sqrt{2}G_F \left(e_L^\dagger \tilde{\sigma}_L^\mu \nu_{eL} \right) \left(\nu_{eL}^\dagger \tilde{\sigma}_{\mu L} e_L \right) \right], \end{aligned} \quad (4)$$

where G_F is the weak Fermi constant, and $\tilde{\sigma}_R^\mu \equiv (\tilde{\sigma}^0, \tilde{\sigma}^1, \tilde{\sigma}^2, \tilde{\sigma}^3)$ and $\tilde{\sigma}_L^\mu \equiv (\tilde{\sigma}^0, -\tilde{\sigma}^1, -\tilde{\sigma}^2, -\tilde{\sigma}^3)$ are respectively the Pauli matrices for the right- and left-handed spinors. By using the Fierz transformation [45], the interacting part of the above action can be given by a neutral current interaction. Hence, we have

$$\tilde{\mathcal{L}}_{\text{int.}} = -2\sqrt{2}G_F \eta_{\hat{a}\hat{b}} \left(e_L^\dagger \sigma_L^{\hat{a}} e_L \right) \left(\nu_{eL}^\dagger \sigma_L^{\hat{b}} \nu_{eL} \right). \quad (5)$$

Note that we have used the fact that $\tilde{\sigma}_L^\mu = \epsilon_a^\mu \sigma_L^{\hat{a}}$, where ϵ_a^μ is the tetrad field. For the solar medium electrons at rest, i.e., non-relativistic, we have

$$e_L^\dagger \sigma_L^{\hat{0}} e_L = e_L^\dagger e_L = \frac{1}{2} n_e(z), \quad (6)$$

where $n_e(z)$ is the number density of electrons inside matter, and the factor 1/2 implies that we only consider the left-handed electrons. It is easy to check out that the expectation value of $e_L^\dagger \sigma_L^i e_L$ is zero.

We predict that the conformal coupling of the neutrino-scalar field can impact the neutrino characteristics and, hence, modify the flavor conversion probabilities. By using the properties of tetrads

$$\tilde{\epsilon}_\mu^a = A(\phi)\epsilon_\mu^a, \quad (7)$$

gamma matrices

$$\tilde{\gamma}^\mu = A^{-1}(\phi)\gamma^\mu, \quad (8)$$

and Christoffel connections

$$\tilde{\Gamma}_{\mu\nu}^\lambda = \Gamma_{\mu\nu}^\lambda - A^{-1}(\phi)A^{\cdot\lambda}(\phi)g_{\mu\nu} + A^{-1}(\phi)A_{,\mu}(\phi)\delta_\nu^\lambda + A^{-1}(\phi)A_{,\nu}(\phi)\delta_\mu^\lambda \quad (9)$$

under the conformal transformation (1), it can be demonstrated that

$$\tilde{\gamma}^\mu \tilde{D}_\mu = A^{-1}(\phi)\gamma^\mu D_\mu + \frac{3}{2}A^{-2}(\phi)A_{,\mu}(\phi)\gamma^\mu, \quad (10)$$

where the second term on the right-hand side is an additional contribution, coming from the conformal coupling to the neutrino action. Thus, the fermionic part action can be written as

$$\begin{aligned} & \int d^4x \sqrt{-\tilde{g}} \left[\bar{\psi}(x) \left(i\tilde{\gamma}^\mu \tilde{D}_\mu - m \right) \psi(x) - \sqrt{2}n_e G_F \bar{\psi}(x)\psi(x) \right] \\ & = \int d^4x \sqrt{-g} \left[\bar{\psi}'(x) \left(i\gamma^\mu D_\mu - m' \right) \psi'(x) - \sqrt{2}n_e G'_F \bar{\psi}'(x)\psi'(x) \right], \end{aligned} \quad (11)$$

provided that the neutrino mass

$$m'(x) = A(\phi)m, \quad (12)$$

the wavefunction

$$\psi'(x) = A^{\frac{3}{2}}(\phi)\psi(x), \quad (13)$$

and the weak Fermi parameter

$$G'_F(x) \equiv A(\phi)G_F, \quad (14)$$

acquire new scalar-dependent forms. We note that $\tilde{g} = A^{2n}(\phi)g$ is the determinant of the spacetime metric denoted by $\tilde{g}_{\mu\nu}$ and n is the number of dimensions. For future considerations, we fix $g_{\mu\nu}$ as the Minkowski metric $\eta_{\mu\nu}$. Also, note that the new form of the adjoint spinor $\bar{\psi}'$ is always the same as the spinor ψ' . Let us now solve the Dirac equation in conformally flat spacetime with rescaled quantities above.

Therefore, after applying the conformal transformation, the matter neutrino action in the conformally flat spacetime is written as

$$\begin{aligned} S_\nu^m &= \int d^4x \sqrt{-g} \left[- \sum_{\alpha,\beta} \nu_{\alpha L}^\dagger m'_{\alpha\beta} \nu'_{\beta R} - \sum_{\alpha,\beta} \nu_{\alpha R}^\dagger m'_{\beta\alpha} \nu'_{\beta L} \right. \\ & \quad \left. + i \sum_\alpha \left(\nu_{\alpha L}^\dagger \sigma_L^\mu \partial_\mu \nu'_{\alpha L} + \nu_{\alpha R}^\dagger \sigma_R^\mu \partial_\mu \nu'_{\alpha R} \right) - V'(z) \nu_{eL}^\dagger \nu'_{eL} \right], \end{aligned} \quad (15)$$

where $V'(z) = \sqrt{2}n_e(z)G'_F(z)$ is the matter potential affected by both SI and NSI of neutrinos. Consider, for instance, the coupling function $A(\phi) = e^{\sigma(\phi)}$ for the chameleon screening model. By assuming $\sigma(\phi) \ll 1$, we can expand the exponential factor in (14) to the first order, which gives

$$\mathcal{L}'_{\text{int.}} = -\sqrt{2}G_F n_e(z) \nu_{eL}^\dagger \nu'_{eL} - \sqrt{2}G_F n_e(z) \sigma(\phi) \nu_{eL}^\dagger \nu'_{eL}. \quad (16)$$

The first term is due to the SI, and the second one with $\sigma(\phi) \propto \phi$ denotes a Yukawa NSI between scalar field and neutrinos.

To obtain the equations of motion for neutrinos traveling inside matter, we take variations of the action (15) with respect to the right- and left-handed spinors:

$$i\sigma_L^\mu \partial_\mu \nu'_{\alpha L} - m'_{\alpha\beta} \nu'_{\beta R} - V'(z) \delta_{\alpha e} \nu'_{eL} = 0, \quad (17)$$

and

$$i\sigma_R^\mu \partial_\mu \nu'_{\alpha R} - m'^*_{\beta\alpha} \nu'_{\beta L} = 0, \quad (18)$$

where $\delta_{\alpha e}$ is the Kronecker delta showing that only matrix elements involving the electron flavor appear in the Hamiltonian. Without losing generality, we define the left-handed and right-handed spinors as follows:

$$\nu'_{\alpha L}(z, t) = e^{-iE(t-t_0)} e^{+iE(z-z_0)} f'_\alpha(z) \begin{pmatrix} 0 \\ 1 \end{pmatrix}, \quad (19)$$

$$\nu'_{\alpha R}(z, t) = e^{-iE(t-t_0)} e^{+iE(z-z_0)} g'_\alpha(z) \begin{pmatrix} 0 \\ 1 \end{pmatrix}. \quad (20)$$

Substituting relations (19) and (20) to the Eqs.(17) and (18) and using the properties of the Pauli matrices lead us to

$$i \frac{df'_\beta(z)}{dz} - m'_{\beta\gamma} g'_\gamma(z) - V'(z) \delta_{\beta e} f'_e(z) = 0, \quad (21)$$

and

$$\left[2E - i \frac{d}{dz} \right] g'_\gamma(z) - m'^*_{\alpha\gamma} f'_\alpha(z) = 0. \quad (22)$$

For neutrinos masses much less than their energies, the second term in the square brackets in Eq.(22), proportional to $\mathcal{O}(m^2/E)$, is negligible with respect to the first one. By applying this approximation, we obtain $g'(z)$ in terms of the function $f'(z)$. Substituting $g'(z)$ to the Eq.(21) and using $m'_{\beta\gamma} = U_{\beta i}^* U_{\gamma i} m'_i$ and unitarity condition $U^{L(R)} U^{L(R)\dagger} = 1$, we obtain the following Schrödinger-like equation of motion in the flavor eigenbasis:

$$i \frac{df'_\beta(z)}{dz} = U_{\alpha i} \left(\frac{m_i'^2}{2E} \right) U_{\beta i}^* f'_\alpha(z) + V'(z) \delta_{\beta e} f'_e(z). \quad (23)$$

Components $U_{\alpha i}$'s are various elements of a unitary matrix called PMNS (Pontecorvo–Maki–Nakagawa–Sakata) matrix:

$$U = \begin{pmatrix} c_{12}c_{13} & s_{12}c_{13} & s_{13}e^{-i\delta} \\ -s_{12}c_{23} - c_{12}s_{23}s_{13}e^{i\delta} & c_{12}c_{23} - s_{12}s_{23}s_{13}e^{i\delta} & s_{23}c_{13} \\ s_{12}s_{23} - c_{12}c_{23}s_{13}e^{i\delta} & -c_{12}s_{23} - s_{12}c_{23}s_{13}e^{i\delta} & c_{23}c_{13} \end{pmatrix}, \quad (24)$$

where $c_{ij} \equiv \cos \theta_{ij}$ and $s_{ij} \equiv \sin \theta_{ij}$, and δ is the Dirac CP-violating phase. We can also write the Eq.(23) in the mass eigenbasis from the relation $f'_i(z) = U_{\alpha i} f'_\alpha(z)$, i.e., we have

$$i \frac{df'_i(z)}{dz} = \frac{m_i'^2}{2E} f'_i(z) + V'(z) U_{ei} U_{ej}^* f'_j(z). \quad (25)$$

Applying the rescaled wavefunction (13) in equation (25), we realize that the effective neutrino Hamiltonian contains both the real and imaginary parts, which are respectively responsible for the modified flavor conversion inside matter and damping behavior caused by NSI. It is more convenient to consider the effective neutrino Hamiltonian as a modification to the masses of neutrinos and determine the resultant mixing parameters in the medium with the effective masses. Then, neutrinos would exactly behave as they do in the

vacuum except possessing different mass and mixing parameters [15]. Therefore, the normalized spacetime part of the neutrino wavefunction can be given by

$$\begin{aligned}\Psi_i(r, t) &= \sqrt{\mathcal{D}_i(r)} e^{-i\varphi_i(r)} \Psi_i(r_0, t_0) \\ &\equiv \mathcal{F}_i(r, t) \Psi_i(r_0, t_0),\end{aligned}\quad (26)$$

where $\varphi_i(r) = \int_{r_0}^r \mathcal{H}_i^{\text{eff}}(r) dr$ is the modified scalar-dependent phase of the neutrino wavefunction. The quantity

$$\mathcal{D}_i(r) \equiv [A_i[\phi(r)] A_i^{-1}[\phi(r_0)]]^{-3} \quad (27)$$

is defined, as a damping or an enhancing factor depending on the treatment of the scalar field ϕ . Ascending ϕ implies the damping factor, and descending field corresponds to the enhancing factor. For notational convenience, we will denote this by \mathcal{D} -factor. Notice that the initial value is satisfied, i.e., $\mathcal{F}_i(r_0, t_0) = 1$.

Without loss of generality, we only focus on the real part of the effective neutrino Hamiltonian. Working at the $\theta_{\text{polar}} = 0$ plane, i.e., $z = r$, and with U as in Eq.(24), the equation (25) in the vacuum mass eigenbasis can be given by

$$i \frac{d}{dr} \begin{pmatrix} \nu_1 \\ \nu_2 \\ \nu_3 \end{pmatrix} = \frac{1}{2E} \begin{pmatrix} \mathcal{A}c_{12}^2 c_{13}^2 & \mathcal{A}c_{12} s_{12} c_{13}^2 & \mathcal{A}c_{12} c_{13} s_{13} \\ \mathcal{A}c_{12} s_{12} c_{13}^2 & \mathcal{A}s_{12}^2 c_{13}^2 + \Delta m_{21}^{\prime 2} & \mathcal{A}s_{12} c_{13} s_{13} \\ \mathcal{A}c_{12} c_{13} s_{13} & \mathcal{A}s_{12} c_{13} s_{13} & \mathcal{A}s_{13}^2 + \Delta m_{31}^{\prime 2} \end{pmatrix} \begin{pmatrix} \nu_1 \\ \nu_2 \\ \nu_3 \end{pmatrix}, \quad (28)$$

where $\mathcal{A}(r) \equiv 2EV'(r)$. To determine the effective mass and mixing parameters induced by the neutrino-scalar NSI inside matter, we should obtain the eigenvalues and eigenvectors of the above Hamiltonian matrix. Of course, the evolution of solar neutrinos within the Sun satisfies the condition $|\Delta m_{31}^{\prime 2}| \gg 2EV'(r)$, which means neutrino flavor transition can be governed by an effective two-neutrino approach, where the evolution of a third eigenstate decouples from the other two [46, 47]. In the next section, we will concentrate on the various probabilities on the Earth, where the detectors have been placed.

3 Damped flavor evolution in matter

The evolved neutrino state corresponding to the flavor α at the spacetime point (t, r) can be suggested as follows:

$$|\nu(\theta, r, t)\rangle_\alpha = \sum_{i, \beta} \mathcal{F}_i(r, t) \Psi_i(r_0, t_0) U_{\beta i}(\theta, r) U_{\alpha i}^*(\theta_M, r_0) |\nu_\beta\rangle, \quad (29)$$

where $U_{\alpha i}(\theta_M, r_0)$ is the (αi) element of the mixing matrix in the matter at the production point and $U_{\beta i}(\theta, r)$ is the (βi) element of the mixing matrix in the vacuum at the detection point. Assume that at (t_0, r_0) , we have a specific flavor neutrino, e.g., ν_α , requires that $\Psi_i(r_0, t_0) = \Psi_0$ for all i 's. Then,

$$P_{\alpha\beta} = \frac{\left| \langle \nu_\beta | \nu(\theta, r, t) \rangle_\alpha \right|^2}{\left| \langle \nu_\alpha | \nu(\theta_M, r_0, t_0) \rangle_\alpha \right|^2} = \left| \sum_i \mathcal{F}_i(r, t) U_{\beta i}(\theta, r) U_{\alpha i}^*(\theta_M, r_0) \right|^2. \quad (30)$$

gives the probability of the flavor transition $\alpha \rightarrow \beta$ on the Earth. For very fast oscillations, the phase parts may be averaged out and, therefore, various probabilities take the forms

$$\langle P_{ee} \rangle = c_{12}^2 c_{13}^2 c_{12}^{M2} c_{13}^{M2} \mathcal{D}_1 + s_{12}^2 c_{13}^2 s_{12}^{M2} c_{13}^{M2} \mathcal{D}_2 + s_{13}^2 s_{13}^{M2} \mathcal{D}_3, \quad (31)$$

$$\begin{aligned}\langle P_{e\mu} \rangle &= \left[s_{12}^2 c_{23}^2 + c_{12}^2 s_{23}^2 s_{13}^2 + \frac{1}{2} \sin 2\theta_{12} \sin 2\theta_{23} s_{13} c_\delta \right] [c_{12}^{M2} c_{13}^{M2}] \mathcal{D}_1 \\ &+ \left[c_{12}^2 c_{23}^2 + s_{12}^2 s_{23}^2 s_{13}^2 - \frac{1}{2} \sin 2\theta_{12} \sin 2\theta_{23} s_{13} c_\delta \right] [s_{12}^{M2} c_{13}^{M2}] \mathcal{D}_2 \\ &+ [s_{23}^2 c_{13}^2] s_{13}^{M2} \mathcal{D}_3,\end{aligned}\quad (32)$$

and $\langle P_{e\tau} \rangle$, which can be obtained by replacing $c_{23} \rightarrow -s_{23}$ and $s_{23} \rightarrow c_{23}$ in Eq.(32). We know that $c_\delta = \cos \delta$. It is worth noting that the total probability $\langle P_{\text{tot.}} \rangle$ is not conserved. In this case, we have $\langle P_{\text{tot.}} \rangle \leq 1$, where the equality holds if and only if the \mathcal{D} -factors are all set to zero.

The probability

$$\delta P_{eX} = 1 - \langle P_{\text{tot.}} \rangle = 1 - \mathcal{D}_1 (c_{12}^{M2} c_{13}^{M2}) - \mathcal{D}_2 (s_{12}^{M2} c_{13}^{M2}) - \mathcal{D}_3 s_{13}^{M2}, \quad (33)$$

can calculate the difference in the total probability from unity. From KamLAND [48], SNO [49], and SK [50] experiments, it is accepted that the mixing between various eigenstates of neutrinos is the most significant reason for the solar neutrino problem. However, all the probabilities above suffer explicitly from damping/enhancing factors denoting an extra deficit in the number of neutrinos on the Earth. This deficit can be considered as a result of a phenomenon called neutrino decay. The subscript X refers to the particle corresponding to the dark energy scalar boson to which neutrinos can decay through the non-standard conformal coupling. As in Ref. [30], such an NSI might modify the neutrino and scalar field density continuity equations, which results in a possible alleviation of the coincidence problem and explains the ignition of the present acceleration of the Universe in the non-relativistic era of mass varying neutrinos (at redshift $z \sim 10$) [25].

As a particular case of interest, suppose that only the lightest neutrino mass eigenstate, ν_1 , is stable during neutrino propagation, i.e., $\mathcal{D}_1 = 1$, and the other two mass states, ν_2 and ν_3 , are coupled to the scalar field. The transition probability of the $\nu_e \rightarrow \phi$ -scalar field is therefore given by

$$\delta P_{e\phi} = 1 - c_{12}^{M2} c_{13}^{M2} - \mathcal{D}_2 (s_{12}^{M2} c_{13}^{M2}) - \mathcal{D}_3 s_{13}^{M2}. \quad (34)$$

In such a case, WEP is violated ($\beta_1 = 0$, whereas $\beta_2, \beta_3 \neq 0$). In dense regions where the scalar field is highly screened, WEP violation may not be detected by local gravitational tests, but there is always the possibility that WEP is violated at the large scales in the chameleon screening model [37, 38, 40]. Furthermore, for small θ_{13}^M , the contribution of ν_3 - ϕ coupling will disappear, i.e., we have

$$\delta P_{e\phi} = (1 - \mathcal{D}_2) s_{12}^{M2}, \quad (35)$$

which increases when \mathcal{D}_2 -factor declines. Experimental constraints on invisible neutrino decay come mainly from the solar and reactor neutrino experiments. A study has been done to look for non-radiative neutrino decay. The strongest constraint on the lifetime of ν_2 is $\tau_2/m_2 > 1.04 \times 10^{-3}$ sec./eV [51].

By way of illustration, we consider a simplified two-flavor case inside matter. Using Eq.(28), the Hamiltonian which governs the propagation of neutrinos inside matter is obtained by

$$\mathcal{H} = \frac{1}{2E} \left[U \begin{pmatrix} m_1'^2 & 0 \\ 0 & m_2'^2 \end{pmatrix} U^\dagger + 2EV'(r) \begin{pmatrix} 1 & 0 \\ 0 & 0 \end{pmatrix} \right]. \quad (36)$$

Hereafter, the important point is to diagonalize the effective Hamiltonian (36) and the derivation of the explicit expressions for the effective oscillation parameters. The solar neutrino parameters of this model correspond to the LMA-MSW solution. It should be recalled that KamLAND [48] has measured the solar mixing angle (θ_{12}) in almost vacuum to be entirely consistent with that from solar experiments such as SNO [49] and SK [50].

After doing some simple calculations, the Hamiltonian above is given by

$$\mathcal{H} = \frac{1}{4E} \left[\Delta m'^2 \begin{pmatrix} -\cos 2\theta & \sin 2\theta \\ \sin 2\theta & \cos 2\theta \end{pmatrix} + 2EV'(r) \begin{pmatrix} 1 & 0 \\ 0 & -1 \end{pmatrix} \right]. \quad (37)$$

Then the effective neutrino oscillation parameters inside matter are

$$\Delta m_M^2 = \sqrt{[\Delta m'^2 \sin 2\theta]^2 + [\Delta m'^2 \cos 2\theta - 2EV'(r)]^2}, \quad (38)$$

and

$$\sin 2\theta_M = \frac{\Delta m'^2 \sin 2\theta}{\Delta m_M^2}. \quad (39)$$

In addition, the damped two-flavor electron-neutrino transition probabilities on the Earth are given by

$$\langle P_{ee} \rangle = \cos^2 \theta \cos^2 \theta_M (\mathcal{D}_1) + \sin^2 \theta \sin^2 \theta_M (\mathcal{D}_2), \quad (40)$$

and

$$\langle P_{e\mu} \rangle = \sin^2 \theta \cos^2 \theta_M (\mathcal{D}_1) + \cos^2 \theta \sin^2 \theta_M (\mathcal{D}_2). \quad (41)$$

Two special cases are investigated: First, if we assume that $\mathcal{D}_1 = \mathcal{D}_2 = \mathcal{D}$, we respect the WEP. We have

$$\begin{aligned} \langle P_{ee} \rangle &= \frac{\mathcal{D}}{2} [1 + \cos 2\theta \cos 2\theta_M], \\ \langle P_{e\mu} \rangle &= \frac{\mathcal{D}}{2} [1 - \cos 2\theta \cos 2\theta_M], \end{aligned} \quad (42)$$

which are the common probabilities multiplied by a \mathcal{D} -factor [52]. Second, if $\mathcal{D}_1 = 1$, but $\mathcal{D}_2 = \mathcal{D} \neq 1$. Then, we have

$$\begin{aligned} \langle P_{ee} \rangle &= \cos^2 \theta \cos^2 \theta_M + \sin^2 \theta \sin^2 \theta_M (\mathcal{D}), \\ \langle P_{e\mu} \rangle &= \sin^2 \theta \cos^2 \theta_M + \cos^2 \theta \sin^2 \theta_M (\mathcal{D}). \end{aligned} \quad (43)$$

This case is devoted to the decay process of the heavier mass eigenstate (ν_2) [11]. As mentioned before, we note that WEP may be violated in such a case.

For neutrinos produced at the center of the Sun, we also consider a phenomenon corresponding to the maximal mixing inside matter, i.e., $\sin 2\theta_M = 1$. The quantity

$$\frac{\Delta m'^2(r_{\text{res.}}) \cos 2\theta}{2\sqrt{2}G'_F(r_{\text{res.}})n_e(r_{\text{res.}})} = E_{\text{res.}}^{\odot} \quad (44)$$

gives the resonance energy. Since the resonance energy is explicitly dependent on the neutrino-scalar coupling functions $A(\phi)$, there would be a shift in the resonance energy for various coupling strengths.

4 Results, discussions and conclusion

A non-standard interaction model of neutrinos has been investigated using the notion of the damped behavior of the neutrino wavefunction through a conformal coupling to the scalar fields. In section 2, the new scalar-dependent forms of the mass, wavefunction, and the *weak Fermi constant* are established for the model in a similar way to those in Ref. [11], in addition, we have obtained the effective Hamiltonian of neutrinos induced by both matter electrons and scalar field. Different exact conversion probabilities have been obtained for *the general 3ν* case in section 3. Deviating from the Standard Model, the sum of various probabilities is assumed not to be equal to unity, which means there exists decay possibility along neutrinos' journey inside matter. Effective mass and mixing parameters due to the interactions with both matter electrons and scalar field are obtained by the diagonalization of the Hamiltonian matrix. It is worth noting that the transition probabilities inside matter are all affected by the \mathcal{D} -factors, and the resonance point energy might be shifted with the various coupling parameter.

Calculations about the chameleon scalar field are performed extensively in the appendix in which a background-object split has been considered. That is, we have expanded the field $\phi(r)$ about its background value ϕ_0 , i.e., $\phi(r) = \phi_0 + \delta\phi(r)$. Figure 7 is plotted for the chameleon field for both constant and exponential density profiles.

Performing the numerical computations in all formulas, one arrives at the results depicted hereafter. Throughout our analysis, we will take the numerical values $n = 1$, and $M \simeq 2.08\text{keV}$ for chameleon [38], and $\tan^2 \theta_{12} = 0.41$, $\sin^2 2\theta_{23} \simeq 0.99$, $\sin^2 2\theta_{13} \simeq 0.09$,

$$\Delta m_{21}^2 = 7.4 \times 10^{-5} \text{eV}^2,$$

and

$$|\Delta m_{23}^2| = 2.5 \times 10^{-3} \text{eV}^2$$

for mass and mixing parameters [53]. In figure 1, we have plotted the survival probability $\langle P_{ee} \rangle$ in terms of the coupling parameter β for the three different values of neutrino energy. As can be seen, all the curves achieve the same value at $\beta \gtrsim 100$.

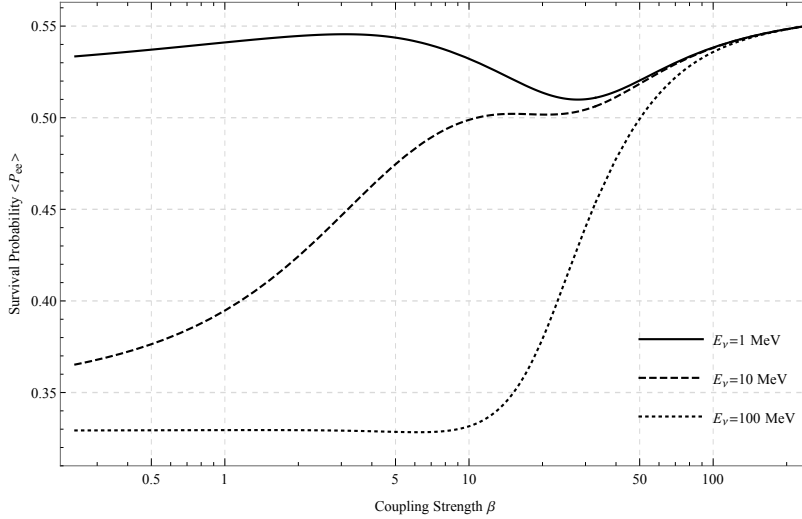


Figure 1: This figure shows the survival probability in terms of the neutrino-scalar coupling parameter β for three neutrino energy. All curves obtain the same values at the $\beta \gtrsim 100$.

Also, the transition probabilities $\langle P_{e\mu} \rangle$ for various neutrino energies $E_\nu \in \{1, 10, 100\}$ MeV are drawn with respect to the parameter β in Fig.2, and these curves show the same treatment at $\beta \gtrsim 100$.

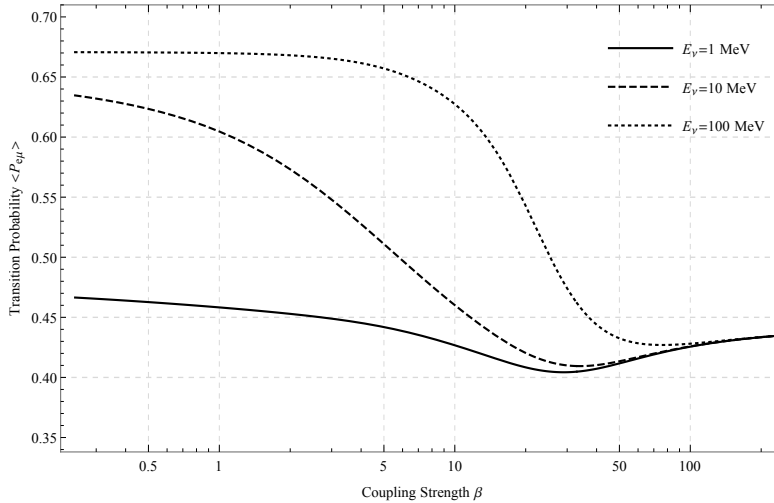


Figure 2: Transition probability in terms of the coupling parameter for different values of neutrino energy. For $\beta \gtrsim 100$, the probability $\langle P_{e\mu} \rangle$ acquires the same value for all energies.

As mentioned earlier, the total probability may not be conserved in the framework of the damped neutrino oscillations. In other words, there would be dissipation in the number of neutrinos received on the Earth, imposed by the \mathcal{D} -factor. Therefore, we defined a loss probability $\delta P_{e\phi}$, which states that the maximum ν_e - ϕ conversion exists at $\beta \simeq 30$, see Fig. 3, as we expected.

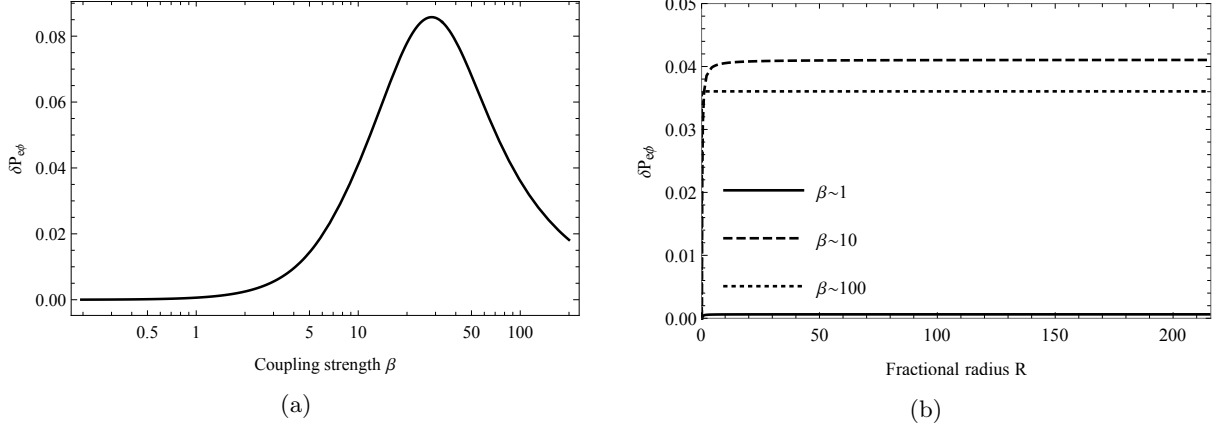


Figure 3: The loss probability of ^8B electron-neutrinos with energy $E_\nu \sim 10$ MeV on the Earth with respect to the coupling parameter β (a), and with respect to the fractional radius R (b). As can be seen, the maximum value belongs to the case with $\beta \simeq 30$. We note that $\delta P_{e\phi} \simeq 0.001$ for $\beta \sim 1$.

We show the effects of the chameleon scalar field NSI on the solar electron-neutrino survival probability in Fig.4. This figure illustrates the LMA-MSW effects on $\langle P_{ee}(E_\nu) \rangle$ for several representative values of β . Also, a comparison with Borexino observational data [41] has been given. As can be seen, the theoretically predicted shift of $\langle P_{ee}(E_\nu) \rangle$ is mostly within the error bars of the experimentally determined values of Borexino. The presence of non-zero coupling parameter β will also shift the resonance energy such that stronger coupling β results in a higher value of $E_{\text{res.}}^\odot$.

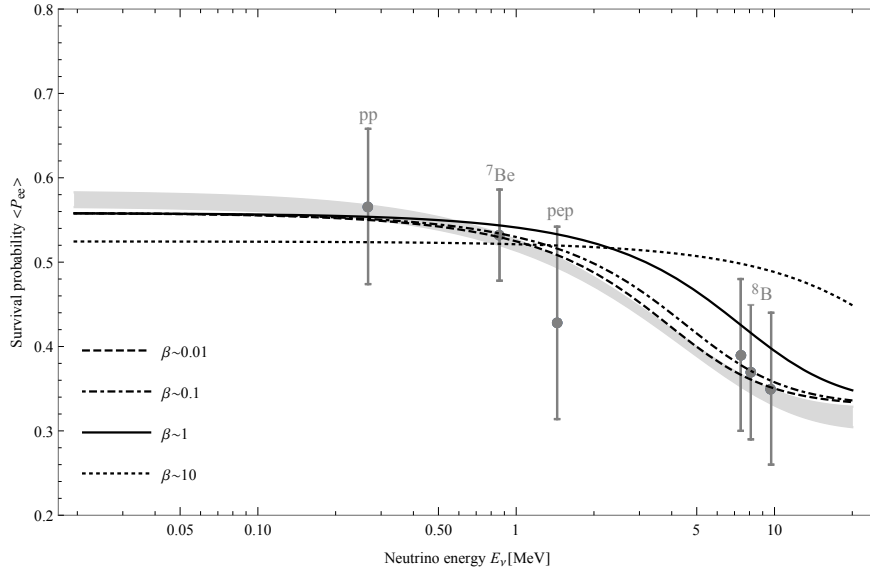


Figure 4: Electron-neutrino survival probability $\langle P_{ee}(E_\nu) \rangle$ as a function of its energy for LMA-MSW case with only SI effects taken into account (gray band), and LMA-MSW + neutrino-scalar NSI cases for $\beta \in \{0.01, 0.1, 1, 10\}$. The data are all taken from Borexino [41].

In Fig.5, we have also depicted the transition probability $\langle P_{e\mu} \rangle$ in terms of the neutrino energy E_ν . The gray curve shows the standard interaction behavior, whereas various curves for the non-standard coupling parameter β are drawn.

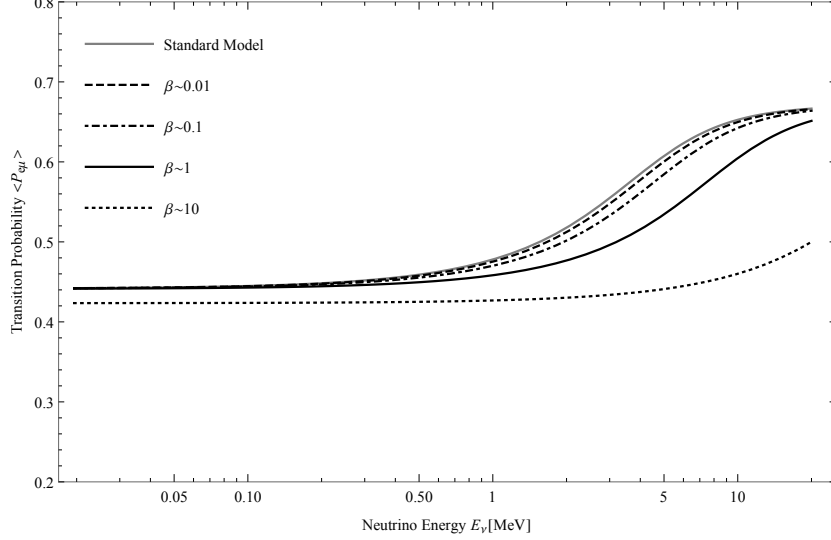


Figure 5: The $\nu_e \rightarrow \nu_\mu$ transition probability with respect to the E_ν . The figure is plotted for both SI and NSI with $\beta \in \{0.01, 0.1, 1, 10\}$.

A Chameleon screening mechanism

The chameleon scalar field is coupled to the different matter species through an exponential conformal factor $A(\phi) = \exp[\beta\phi/M_p]$ with an inverse-power law potential

$$V(\phi) = M^{4+n} \phi^{-n}. \quad (\text{A.1})$$

Here, β is the scalar-matter coupling constant, n is a positive number, and M is the parameter of mass scale.

Variation from the action (2) with respect to the field ϕ gives the equation of motion

$$\square\phi = V_{,\phi} - A^3(\phi)A_{,\phi}(\phi)\tilde{g}^{\mu\nu}\tilde{T}_{\mu\nu}, \quad (\text{A.2})$$

where $\tilde{T}_{\mu\nu} \equiv (-2/\sqrt{\tilde{g}})\delta\mathcal{L}_m/\delta\tilde{g}_{\mu\nu}$ is the energy-momentum tensor of matter components [37, 40]. For non-relativistic matter, Eq.(A.2) yields

$$\square\phi = V_{\text{eff.},\phi}, \quad (\text{A.3})$$

where $V_{\text{eff.},\phi}(\phi) = V_{,\phi}(\phi) + A_{,\phi}(\phi)\rho$ is the effective potential, which governs the dynamics of the scalar field. The most critical ingredient in the chameleon field model is the minimum of the effective potential, i.e.,

$$\phi_{\text{min.}} = \left[\frac{nM^{4+n}M_p}{\beta\rho} \right]^{\frac{1}{n+1}}, \quad (\text{A.4})$$

and the mass of fluctuations around the minimum, i.e.,

$$m_{\text{min.}}^2 = \frac{n(n+1)M^{4+n}}{\phi_{\text{min.}}^{n+2}} + \frac{\rho\beta^2}{M_p^2}, \quad (\text{A.5})$$

both depend explicitly on the ambient matter density ρ . Expanding the scalar field around its background value up to linear order, i.e., $\phi(r) = \phi_0 + \delta\phi(r)$, allows us to reduce Eq.(A.3) to an equation for the perturbative part

$$\frac{d^2\delta\phi}{dr^2} + \frac{2}{r}\frac{d\delta\phi}{dr} - m_{\text{min.}}^2(\phi_0)\delta\phi = \frac{\beta(\phi_0)}{M_p}\rho(r), \quad (\text{A.6})$$

where the source $\rho(r)$ on the right-hand side imposes matter effects in the scalar field. We assume that the mass density inside the Sun can be described by an exponential function, as shown in Fig.6:

$$\rho(R) = \begin{cases} \rho_c e^{-\lambda R_\odot R} & (R \leq 1) \\ \rho_0 & (R > 1) \end{cases}, \quad (\text{A.7})$$

where the parameter λ is considered a positive constant, and R_\odot and $R \equiv r/R_\odot$ are the solar and dimensionless fractional radii, respectively.

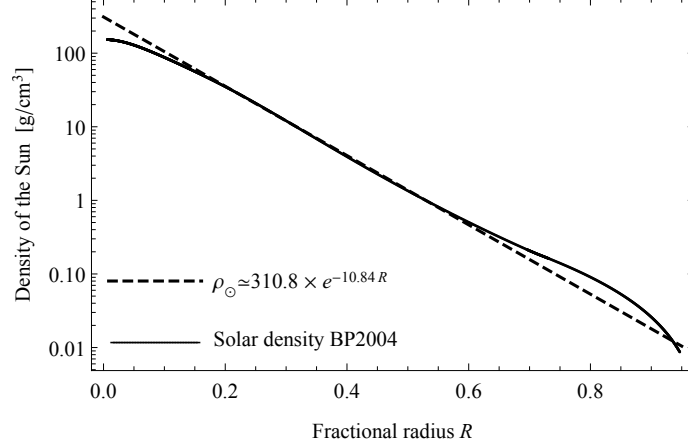


Figure 6: Solar density distribution function in terms of the dimensionless fractional radius R . This figure is plotted by BP2004 data [54].

We can find a solution analytically to the scalar field equation (A.6) inside and outside the Sun placed in a medium with constant matter density ρ_0 . Thus; we have

$$\begin{aligned} \delta\phi_{\text{in}}(R) = & \frac{e^{-(\lambda+2m_{\text{in}})R_\odot R}}{2m_{\text{in}}M_p R_\odot (m_{\text{in}}^2 - \lambda^2)^2 R} \left[C_1 M_p (m_{\text{in}}^2 - \lambda^2)^2 (e^{2m_{\text{in}}R_\odot R} - 1) e^{(\lambda+m_{\text{in}})R_\odot R} \right. \\ & \left. + 2\beta m_{\text{in}} \rho_c \left(e^{2m_{\text{in}}R_\odot R} (2\lambda + (\lambda^2 - m_{\text{in}}^2) R_\odot R) - 2\lambda e^{(\lambda+m_{\text{in}})R_\odot R} \right) \right], \quad (R < 1) \end{aligned} \quad (\text{A.8})$$

and

$$\delta\phi_{\text{out}}(R) = C_2 \frac{e^{-m_{\text{out}}R_\odot R}}{R}. \quad (R > 1) \quad (\text{A.9})$$

To obtain the integration constants, we apply the boundary conditions

$$\begin{aligned} \frac{d\delta\phi}{dR} &= 0 \quad \text{at} \quad R \rightarrow 0, \\ \delta\phi &\rightarrow 0 \quad \text{at} \quad R \rightarrow \infty, \end{aligned} \quad (\text{A.10})$$

and the continuity conditions at the solar surface $R = 1$. By assuming $m_{\text{in}}R_\odot \gg 1$ and $m_{\text{out}}R_\odot \ll 1$, we fix these two constants as follows:

$$C_1 = \frac{2\beta\rho_c e^{-2m_{\text{in}}R_\odot}}{M_p (m_{\text{in}}^2 - \lambda^2)^2} \left[e^{(m_{\text{in}} - \lambda)R_\odot} (m_{\text{in}}^2 (1 - \lambda R_\odot) + \lambda (\lambda - m_{\text{out}} (\lambda R_\odot + 2) + \lambda^2 R_\odot)) - 2\lambda m_{\text{in}} \right], \quad (\text{A.11})$$

and

$$\begin{aligned} C_2 = & \frac{\beta\rho_c e^{-(2m_{\text{in}} + \lambda)R_\odot}}{M_p m_{\text{in}} R_\odot (m_{\text{in}}^2 - \lambda^2)^2} \left[-m_{\text{in}}^3 R_\odot e^{2m_{\text{in}}R_\odot} - m_{\text{in}}^2 (\lambda R_\odot - 1) e^{2m_{\text{in}}R_\odot} \right. \\ & \left. + \lambda^2 (\lambda R_\odot + 1) e^{2m_{\text{in}}R_\odot} + \lambda m_{\text{in}} \left((\lambda R_\odot + 2) e^{2m_{\text{in}}R_\odot} - 4e^{(\lambda+m_{\text{in}})R_\odot} \right) \right]. \end{aligned} \quad (\text{A.12})$$

As a particular case of interest, by setting $\lambda \rightarrow 0$, all above relations can be re-written for constant or slowly varying matter density ρ_c . Now, we can plot the treatment of the scalar field in terms of the dimensionless fractional radius R . Figure 7 shows the chameleon scalar field for $\beta \sim 1$ and two various cases: the constant and exponential densities. As can be seen, both curves show different behaviors inside the Sun but tend to an asymptotic value outside it.

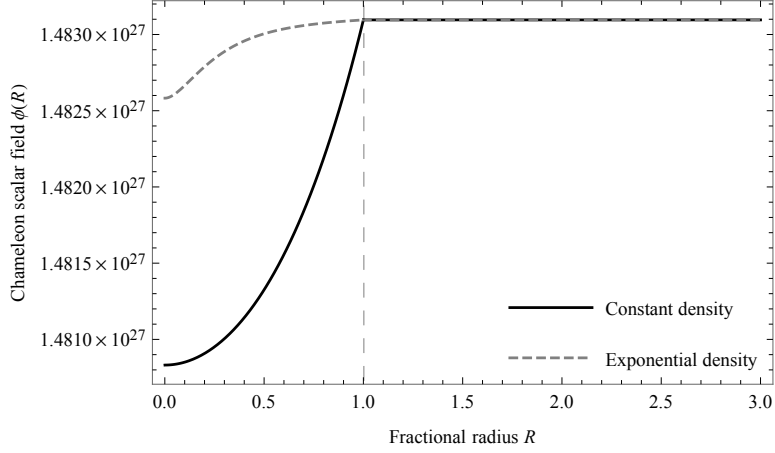


Figure 7: This figure shows how the scalar field is affected by the matter density $\rho(R)$. We have assumed that $\beta \sim 1$.

On the other side, we can see how the coupling parameter β can impact the chameleon scalar field. As shown in Fig.8, the field ϕ chooses smaller asymptotic values when β increases.

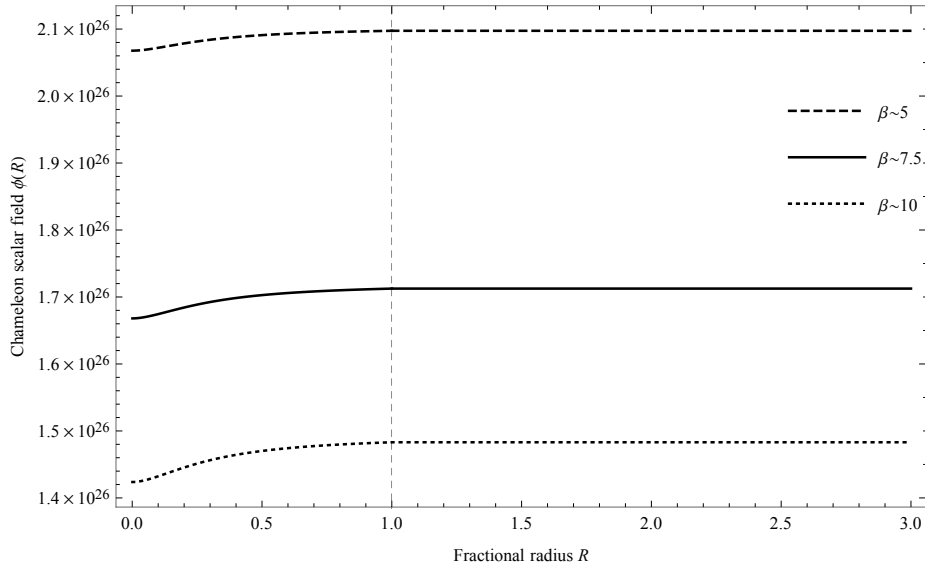


Figure 8: The chameleon scalar field for three different values of the coupling strengths $\beta \in \{5, 7.5, 10\}$. The field, in each case, approaches an asymptotic value outside the body, which increases with decreasing β . The field values are all in eV.

References

- [1] Y. Fukuda *et al.* [Super-Kamiokande], Nucl. Instrum. Meth. A **501**, 418-462 (2003).

- [2] Q. R. Ahmad *et al.* [SNO], Phys. Rev. Lett. **89**, 011301 (2002) [arXiv:nucl-ex/0204008 [nucl-ex]].
- [3] A. Gando *et al.* [KamLAND], Phys. Rev. D **88**, no.3, 033001 (2013) [arXiv:1303.4667 [hep-ex]].
- [4] C. Y. Cardall and G. M. Fuller, Phys. Rev. D **55**, 7960-7966 (1997) [arXiv:hep-ph/9610494 [hep-ph]].
- [5] N. Fornengo, C. Giunti, C. W. Kim and J. Song, Phys. Rev. D **56**, 1895 (1997) [arXiv:hep-ph/9611231 [hep-ph]].
- [6] L. Visinelli, Gen. Rel. Grav. **47**, 62 (2015) [arXiv:1410.1523 [gr-qc]].
- [7] S. Chakraborty, JCAP **10**, 019 (2015) [arXiv:1506.02647 [gr-qc]].
- [8] H. Mohseni Sadjadi and A. P. Khosravi, JCAP **04**, 008 (2018) [arXiv:1711.06607 [hep-ph]].
- [9] M. Blasone, G. Lambiase, G. G. Luciano and L. Petruzziello, EPL **124**, 51001 (2018) [arXiv:1812.09697 [hep-ph]].
- [10] L. Buoninfante, G. G. Luciano, L. Petruzziello and L. Smaldone, Phys. Rev. D **101**, 024016 (2020) [arXiv:1906.03131 [gr-qc]].
- [11] H. Mohseni Sadjadi and H. Y. Ahmadabadi, Phys. Rev. D **103**, 065012 (2021) [arXiv:2012.03633 [hep-ph]].
- [12] H. Y. Ahmadabadi and H. M. Sadjadi, “Screening models and neutrino oscillations,” [arXiv:2111.03054 [hep-ph]].
- [13] L. Wolfenstein, Phys. Rev. D **20**, 2634 (1979).
- [14] S. P. Mikheyev, A. Yu. Smirnov, Sov. J. Nucl. Phys. **42**, 913 (1985).
- [15] Y. H. Zhang and X. Q. Li, Nucl. Phys. B **911**, 563-581 (2016) [arXiv:1606.05960 [hep-ph]].
- [16] O. G. Miranda and H. Nunokawa, New J. Phys. **17**, no.9, 095002 (2015) [arXiv:1505.06254 [hep-ph]].
- [17] S. F. Ge and S. J. Parke, Phys. Rev. Lett. **122**, no.21, 211801 (2019) [arXiv:1812.08376 [hep-ph]].
- [18] P. S. Bhupal Dev, K. S. Babu, P. B. Denton, P. A. N. Machado, C. A. Argüelles, J. L. Barrow, S. S. Chatterjee, M. C. Chen, A. de Gouvêa and B. Dutta, *et al.* SciPost Phys. Proc. **2**, 001 (2019) [arXiv:1907.00991 [hep-ph]].
- [19] L. Amendola, M. Baldi and C. Wetterich, Phys. Rev. D **78**, 023015 (2008) [arXiv:0706.3064 [astro-ph]].
- [20] A. W. Brookfield, C. van de Bruck, D. F. Mota and D. Tocchini-Valentini, Phys. Rev. Lett. **96**, 061301 (2006) [arXiv:astro-ph/0503349 [astro-ph]].
- [21] M. Carrillo González, Q. Liang, J. Sakstein and M. Trodden, JCAP **04**, 063 (2021) [arXiv:2011.09895 [astro-ph.CO]].
- [22] S. Mandal, G. Y. Chitov, O. Avsajanishvili, B. Singha and T. Kahniashvili, JCAP **05**, 018 (2021) [arXiv:1911.06099 [hep-ph]].
- [23] J. G. Salazar-Arias and A. Pérez-Lorenzana, Phys. Rev. D **101**, no.8, 083526 (2020) [arXiv:1907.00131 [hep-ph]].
- [24] A. R. Khalifeh and R. Jimenez, Phys. Dark Univ. **31**, 100777 (2021) [arXiv:2010.08181 [gr-qc]].
- [25] R. Fardon, A. E. Nelson and N. Weiner, JCAP **10**, 005 (2004) [arXiv:astro-ph/0309800 [astro-ph]].
- [26] P. Gu, X. Wang and X. Zhang, Phys. Rev. D **68**, 087301 (2003) [arXiv:hep-ph/0307148 [hep-ph]].
- [27] V. Barger, P. Huber and D. Marfatia, Phys. Rev. Lett. **95**, 211802 (2005) [arXiv:hep-ph/0502196 [hep-ph]].

- [28] M. Cirelli, M. C. Gonzalez-Garcia and C. Pena-Garay, Nucl. Phys. B **719**, 219-233 (2005) [arXiv:hep-ph/0503028 [hep-ph]].
- [29] C. Wetterich, Phys. Lett. B **655**, 201-208 (2007) [arXiv:0706.4427 [hep-ph]].
- [30] H. Mohseni Sadjadi and V. Anari, Phys. Rev. D **95**, no.12, 123521 (2017) [arXiv:1702.04244 [gr-qc]].
- [31] H. M. Sadjadi and V. Anari, JCAP **10**, 036 (2018) [arXiv:1808.01903 [gr-qc]].
- [32] D. B. Kaplan, A. E. Nelson and N. Weiner, Phys. Rev. Lett. **93**, 091801 (2004) [arXiv:hep-ph/0401099 [hep-ph]].
- [33] R. Bean, E. E. Flanagan and M. Trodden, Phys. Rev. D **78**, 023009 (2008) [arXiv:0709.1128 [astro-ph]].
- [34] H. Mohseni Sadjadi, M. Honardoost and H. R. Sepangi, Phys. Dark Univ. **14**, 40-47 (2016) [arXiv:1504.05678 [gr-qc]].
- [35] M. Honardoost, H. Mohseni Sadjadi and H. R. Sepangi, Gen. Rel. Grav. **48**, no.10, 125 (2016) [arXiv:1508.06022 [gr-qc]].
- [36] J. Khoury and A. Weltman, Phys. Rev. Lett. **93**, 171104 (2004) [arXiv:astro-ph/0309300 [astro-ph]].
- [37] J. Khoury and A. Weltman, Phys. Rev. D **69**, 044026 (2004) [arXiv:astro-ph/0309411 [astro-ph]].
- [38] T. P. Waterhouse, “An Introduction to Chameleon Gravity,” [arXiv:astro-ph/0611816 [astro-ph]].
- [39] S. Tsujikawa, T. Tamaki and R. Tavakol, JCAP **05**, 020 (2009) [arXiv:0901.3226 [gr-qc]].
- [40] C. Burrage and J. Sakstein, Living Rev. Rel. **21**, no.1, 1 (2018) [arXiv:1709.09071 [astro-ph.CO]].
- [41] M. Agostini *et al.* [BOREXINO], Nature **562**, no.7728, 505 (2018).
- [42] V. Faraoni, E. Gunzig and P. Nardone, Fund. Cosmic Phys. **20**, 121 (1999) [arXiv:gr-qc/9811047 [gr-qc]].
- [43] D. F. Carneiro, E. A. Freiras, B. Goncalves, A. G. de Lima and I. L. Shapiro, Grav. Cosmol. **10**, 305-312 (2004) [arXiv:gr-qc/0412113 [gr-qc]].
- [44] W. N. Cottingham and D. A. Greenwood, “An Introduction to the Standard Model of Particle Physics,” Cambridge university press, ISBN-13 978-0-521-85249-4, 2007.
- [45] M. Fierz, Zur fermi sohen theorie des β -zerfalls, Z. Phys. **104** (1937) 553; J. F. Nieves and P. B. Pal, Am. J. Phys. **72**, 1100-1108 (2004) [arXiv:hep-ph/0306087 [hep-ph]].
- [46] S. K. Agarwalla *et al.* [Borexino], JHEP **02**, 038 (2020) [arXiv:1905.03512 [hep-ph]].
- [47] P. Martínez-Miravé, S. M. Sedgwick and M. Tórtola, [arXiv:2111.03031 [hep-ph]].
- [48] A. Gando *et al.* [KamLAND], Phys. Rev. D **88**, no.3, 033001 (2013) [arXiv:1303.4667 [hep-ex]].
- [49] B. Aharmim *et al.* [SNO], Phys. Rev. C **88**, 025501 (2013) [arXiv:1109.0763 [nucl-ex]].
- [50] J. Hosaka *et al.* [Super-Kamiokande], Phys. Rev. D **73**, 112001 (2006) [arXiv:hep-ex/0508053 [hep-ex]]; J. P. Cravens *et al.* [Super-Kamiokande], Phys. Rev. D **78**, 032002 (2008) [arXiv:0803.4312 [hep-ex]]; K. Abe *et al.* [Super-Kamiokande], Phys. Rev. D **83**, 052010 (2011) [arXiv:1010.0118 [hep-ex]]; K. Abe *et al.* [Super-Kamiokande], Phys. Rev. D **94**, no.5, 052010 (2016) [arXiv:1606.07538 [hep-ex]].
- [51] B. Aharmim *et al.* [SNO], Phys. Rev. D **99**, no.3, 032013 (2019) [arXiv:1812.01088 [hep-ex]].
- [52] M. C. Gonzalez-Garcia and Y. Nir, Rev. Mod. Phys. **75**, 345-402 (2003) [arXiv:hep-ph/0202058 [hep-ph]].
- [53] I. Esteban, M. C. Gonzalez-Garcia, M. Maltoni, T. Schwetz and A. Zhou, JHEP **09**, 178 (2020) [arXiv:2007.14792 [hep-ph]]; see also www.nu-fit.org.
- [54] J. N. Bahcall and M. H. Pinsonneault, Phys. Rev. Lett. **92**, 121301 (2004) [astro-ph/0402114].